Mapping the spin-dependent electron reflectivity of Fe and Co ferromagnetic thin films

J. Graf,[1,*] C. Jozwiak,[2] A.K. Schmid,[1] Z. Hussain,[3] and A. Lanzara[1,2]

[1] *Materials Sciences Division, Lawrence Berkeley National Laboratory, Berkeley, California 94720*
[2] *Dept. of Physics, University of California Berkeley, California 94720*
[3] *Advanced Light Source, Lawrence Berkeley National Laboratory, Berkeley, California 94720*

(Dated: February 2, 2008)

Spin Polarized Low Energy Electron Microscopy is used as a spin dependent spectroscopic probe to study the spin dependent specular reflection of a polarized electron beam from two different magnetic thin film systems: Fe/W(110) and Co/W(110). The reflectivity and spin-dependent exchange-scattering asymmetry are studied as a function of electron kinetic energy and film thickness, as well as the time dependence. The largest value of the figure of merit for spin polarimetry is observed for a 5 monolayer thick film of Co/W(110) at an electron kinetic energy of 2eV. This value is 2 orders of magnitude higher than previously obtained with state of the art Mini-Mott polarimeter. We discuss implications of our results for the development of an electron-spin-polarimeter using the exchange-interaction at low energy.

Keywords: exchange scattering; Co/W(110); Fe/W(110); ferromagnetic thin film; electron spin polarimeter; figure of merit; SPLEEM; Sherman function

I. INTRODUCTION

State of the art electron spectrometers have reached an energy and momentum resolution that allows probing subtle and complex many-body effects. However the low efficiency of spin-detection impedes experimental progress towards our improved understanding of the spin degree of freedom in complex and magnetic materials. In terms of spin-detector development, a quantity of great interest is defined as the Figure of Merit (FOM) and is proportional to the inverse square of the statistical error in an electron counting experiment to measure the polarization of an incident beam[1]. Conventional spin-polarimeters (mini-Mott detectors) have a FOM below $2\text{x}10^{-4}$ [2]. This low FOM has long been recognized as problematic. For well over one decade, various groups have worked on the idea to use exchange-scattering of low energy electrons by ferromagnetic surfaces as a promising route toward achieving significantly improved efficiency. For example, detailed investigations of Fe(110) surface have shown that FOM of the order of $8\text{x}10^{-3}$ can be achieved [3,6]. Along this direction, different surfaces have been investigated to increase the FOM, the lifetime and the reproducibility[4,5]. Recently, FOM up to $6\text{x}10^{-3}$ have been achieved with a robust system, Fe(001)-p(1x1)O[7,8], and a spin resolved electron spectrometer has been built [9]. A different approach suggested even higher FOM (up to $5\text{x}10^{-2}$) using high quality ultra-thin Co or Fe films on W(110)[10,11]. Unfortunately, the microscopic size of this ultra-thin film is problematical in spin polarimetry applications[9]. Here, we demonstrate that a larger film of lower quality that can be easily grown and reproduced at room temperature can indeed reliably achieve very high FOM.

In this paper, we report a detailed study of the reflectivity and spin-dependent exchange-scattering asymmetry as a function of electron kinetic energy and film thickness and as a function of time for two different magnetic thin film systems grown at room temperature: Fe/W(110) and Co/W(110). The results confirm the possibility of constructing novel spin polarimeters with FOM up to two orders of magnitude higher than state of the art mini-Mott polarimeter and stray fields significantly lower than current exchange-scattering-based polarimeters using bulk ferromagnets.

II. EXPERIMENTAL TECHNIQUE

The data reported here are taken with a Spin Polarized Low Energy Electron Microscope (SPLEEM)[12] located in the National Center for Electron Microscopy of the Lawrence Berkeley National Laboratory. SPLEEM is a powerful tool to image the dynamics of surface magnetic microstructures in the sub-second timescale, and its sensitivity to the sample surface allows the imaging of atomic steps with a lateral resolution of ∼20nm. Here, we use it as a fast and powerful spin dependent electronic probe by recording the number of elastically backscattered electrons as a function of their spin and energy.

Cobalt and iron films were prepared at room temperature by electron beam evaporation of high-purity material on a (110) tungsten crystal. The tungsten substrate was cleaned by successive flash heating cycles in an O_2 environment of 10^{-8} Torr, followed by flash heating in UHV up to ≈2000°C. The substrate cleanliness was monitored by Auger electron spectroscopy and no traces of contamination were detected. The base pressure was on the order of 10^{-11} Torr and was in the low 10^{-10} Torr region during film deposition. The deposition rate was measured by direct observation with SPLEEM and adjusted to approximately 0.1 monolayer (ML) per minute. Both Co and Fe grow in a quasi layer-by-layer mode at room temperature as previously reported[13,14].

More specifically, Fe grows in a pseudomorphic mode for the first 1.8 ML, and then relaxes to a bulk bcc structure. The cobalt film adopts pseudomorphic structure for the first ML and then transforms to a close-packed structure[15].

Figures 1a and b show images of the magnetic surface for Co/W(100) (1a) and Fe/W(110) (1b) at a certain energy and film thickness. The bright areas represent flat terraces on the crystal surface and the darker curving lines and bands represent the monoatomic steps and multilayer step bands of the W(110) surface. A blue and a red region can be observed for both images. These two regions represent two magnetic domains with opposite magnetization (black arrows). The white arrows represent the majority spin orientation of the illumination electron beam. Within the imaged field of view, regions of interest (ROI) where substrate step-density is low and film magnetization is homogeneously aligned in a particular magnetic domain (see black contour in figure 1a and b) are selected. The average intensity at a given electron energy, film thickness and spin orientation is extracted in these regions. The spin-polarization of the illuminating electron beam was adjusted to be aligned with the magnetic easy axis of the film. Continuous sequences of images of the surfaces were then recorded automatically, during the simultaneous deposition of the ferromagnetic thin films. For each set of two consecutive images, the spin orientation of the electron beam was toggled to be parallel and anti-parallel to the film magnetization. The deposition rate was adjusted to be sufficiently slow so that during the deposition of each ML we were able to ramp several times the electron beam energy from 0 to 13 eV in steps of 0.2 eV (with respect to the vacuum level). The average intensity in the selected ROI is then measured for each image and normalized with respect to the electron illumination intensity.

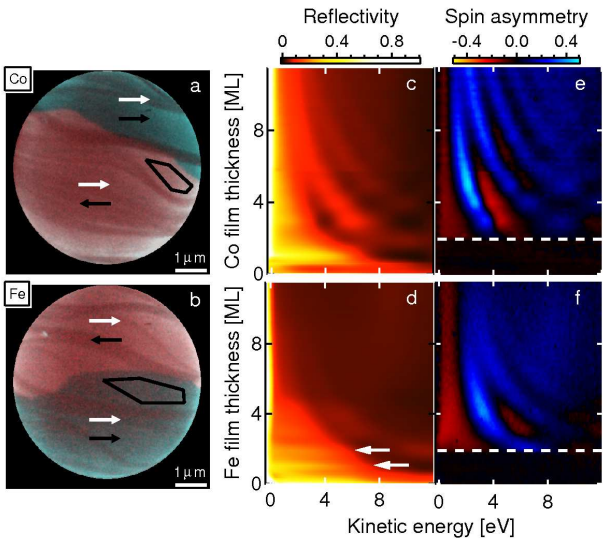

FIG. 1: (Color online) Panels (a) and (b) show SPLEEM images of Co/W(110) and Fe/W(110) films, respectively. For both films the magnetic easy axis points along the horizontal direction in the images. Both images were recorded with electron spin polarization aligned to the right (white arrow). The magnetic domains are shown with blue and red contrast, magnetization direction of the domains is indicated by black arrows. Black contours are the regions of interest for average reflectivity measurements. (c,d) Color-scale plots of the measured reflectivity as a function of the electron kinetic energy (horizontal axis) and film thickness (vertical axis) for both thin-film systems. (e,f) Color-scale plots of the spin asymmetry of the reflectivity.

III. RESULTS

Figure 1c (d) shows a color plot representing the average reflectivity for cobalt (iron) versus the electron energy (horizontal axis) and the film thickness (vertical axis). The variations in the reflectivity seem to have at least two periodic components. The component that is visibly energy independent (see white arrows in fig. 1d) is due to the varying density of steps during deposition. The reflectivity minima (in black) coincide with half completed monolayers (higher surface step density) and the maxima (in red) occur with the completion of each monolayer (low surface step density). These growth oscillations are most clear at small film thickness and are used to calibrate the film deposition rate. The interesting component is energy dependent and looks like hyperbolic shaped maxima (in red) and minima (in black) in the reflectivity plots (more pronounced for Co/W(100)). This is a bulk and intrinsic effect known as the "Quantum Size Effect" (QSE)[10,16]. More specifically, a ferromagnetic slab acts like a resonant cavity and induces interference patterns. The QSE is more pronounced for Co/W(110) (fig. 1c) than for Fe/W(110) (fig. 1d) films. We attribute this attenuation to previously reported kinetic roughening during room temperature growth of Fe/W(110)[10].

In figure 1e and f, we report the spin asymmetry versus energy and film thickness for Co/W(110) and Fe/W(110) films respectively. Here, the spin asymmetry (or Sherman function) is defined by

$$A_s = \frac{1}{P}\frac{R_{\uparrow\downarrow} - R_{\uparrow\uparrow}}{R_{\uparrow\downarrow} + R_{\uparrow\uparrow}}$$

where P is the polarization of the electron beam (20%) and $R_{\uparrow\uparrow}$ ($R_{\uparrow\downarrow}$) is the reflectivity for electrons with spin parallel (anti-parallel) to the magnetization of the film. The white dashed lines at 2 ML film thickness in figure 1e and f clearly separate a uniform black region from a modulated red and blue region. The featureless black region indicates a perfect symmetry in both Fe and Co films reflectivity. This can be explained by noting that the Curie temperature (T_c) of Fe/W(110) films is above room temperature only for film thickness greater than 2 ML[17]. We attribute the absence of spin asymmetry in thin Co films to a similar depression of the Curie temperature. The remarkably perfect symmetry of the mea-

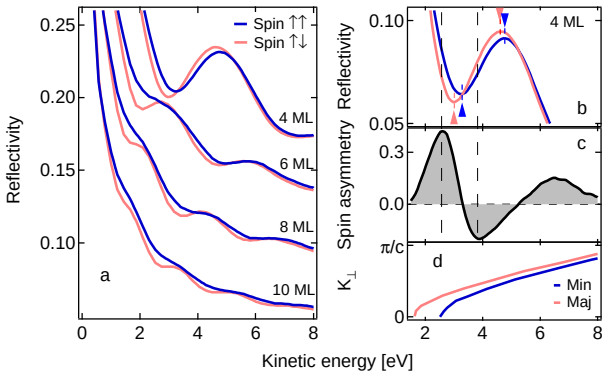

FIG. 2: (Color online) (a) Energy dependence of the reflectivity for spin parallel and anti-parallel to the Co/W(110) film magnetic axis for different film thickness. The energy scans are incrementally shifted by 0.05. (b) Expanded view of the spin dependence of the reflectivity for the 4 ML thick film. (c) Spin asymmetry for a 4 ML thick Co/W(110) film obtained from fig 1b. (d) Band structure calculation for a 4 ML thick Co/W(110) film[16].

surement above T_c supports the magnetic origin of the asymmetry measured below T_c.

Figure 2a shows energy scans of the spin dependent reflectivity for different Co film thicknesses. For each film thickness, two main observations can be made about the spin dependent reflectivity:

1. The reflectivity for the anti-parallel spin (red curve) shows a red shift with respect to the case of parallel spin (blue curve).

2. The reflectivity oscillation in the case of spin parallel (blue curve) are damped with respect to the anti-parallel spin case (red curve).

These observations suggest that two mechanisms contribute to the total spin asymmetry. The spectra for film thickness bigger than 5-6 ML are mainly dominated by the damping mechanism. We attribute the damping to different mean free paths for spin parallel or anti-parallel to the majority spin. Indeed it is known that the so-called universal curve predicts too large a value of the inelastic mean free path (IMFP) for transition metals at low energy, and spin dependent values of the IMFP corresponding to a few monolayers have been reported at the energies considered in this paper[18,19,20]. These results suggests that SPLEEM can be used as a tool to extract information on the spin dependent mean free path, a fundamental quantity for many properties of solids. A more detailed study is required.

The red shift of the anti-parallel spin reflectivity spectra can be clearly observed in figure 2b, where the spin dependent reflectivity for a 4 ML thick Co/W(110) film is shown. We see that the large gradients of the reflectivity induced by the quantum well states are slightly shifted for electrons of opposite spin due to the exchange splitting of the band structure. The minima and the maxima

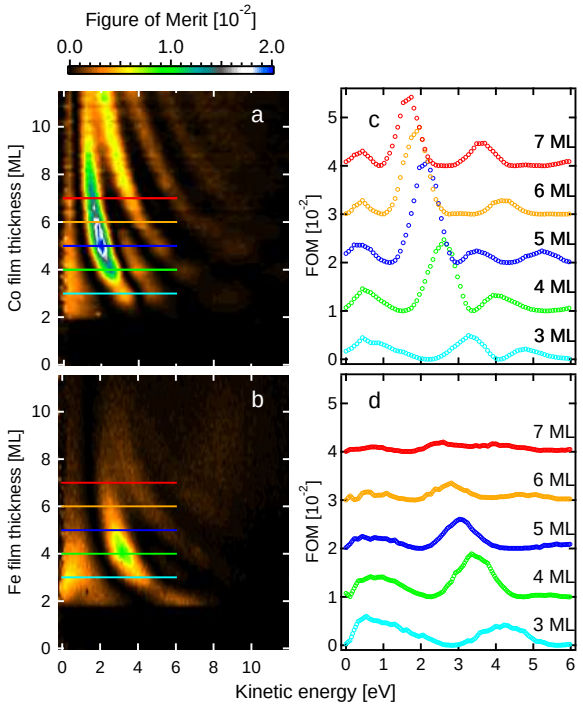

FIG. 3: (Color online) (a,b) Color-scale plots of the "figure of merit" for Co/W(110) and Fe/W(110) thin films respectively, as a function of the electron kinetic energy (horizontal axis) and film thickness (vertical axis). (c,d) The respective figure of merit, plotted as a function of energy for Co and Fe at different thicknesses. For clarity, the energy scans are incrementally shifted by 10^{-2}. The location of the scans is shown by color horizontal lines in panel a and b.

of the reflectivity indicated with the blue and red arrow are shifted by 0.3 eV and 0.15 eV respectively. It is the combination of this energy shift with the large gradients in the reflectivity that causes significant enhancement or reduction of the magnetic asymmetry as shown in figure 2c. This seems to be the dominant mechanism at small film thickness even in the presence of some inelastic damping.

Figure 2d shows a band structure calculation along the perpendicular direction for a 4 ML Co/W(110) thin film[16]. From the band structure calculation and the measured spin asymmetry, one can see that the first maxima at 2.6 eV of the spin asymmetry may have a contribution from the exchange-split band gap. But there is no band gap at the second maxima at 4.7 eV and one can see again the strong contribution of the finite size at small film thickness.

In figures 3a and b, the dependence of the figure of merit (FOM) on electron kinetic energy (horizontal axis) and film thickness (vertical axis) for Co/W(110) and Fe/W(110) is shown. The figure of merit combines the reflectivity and the spin asymmetry and is defined by $A_s^2 \frac{R_{\uparrow\downarrow}+R_{\uparrow\uparrow}}{2}$. This whole map of the figure of merit emphasizes the important role of the QSE oscillations for

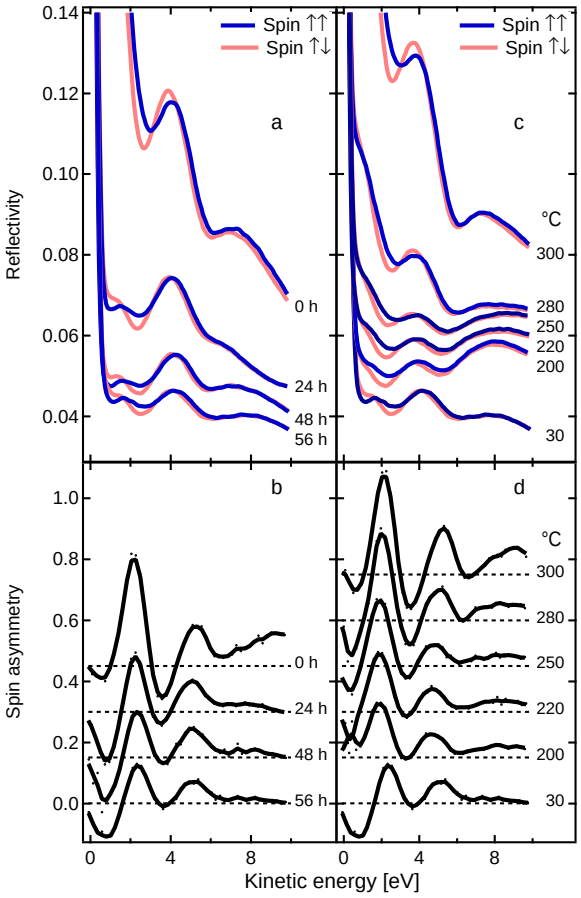

FIG. 4: (Color online) Aging effects and regeneration for a 5 ML thick cobalt film: (a) Evolution of the reflectivity of the film with time in UHV conditions. Red (blue) energy scans represent incident electrons with spin polarization parallel (anti-parallel) to the magnetization. For clarity, each curve is shifted by 0.01. (b) The spin asymmetry calculated from the reflectivity distribution curves in panel (a). The effect of annealing on the reflectivity and the corresponding spin asymmetry are shown in (c) and (d), respectively, after 56 hours of room-temperature aging in UHV.

spin detection. The FOM is in fact very sensitive to the film thickness and electron energy. A maximum for the FOM is reached only in a narrow range of energy and film thickness. This feature must be taken into account for further development of electron spin polarimetry. In figure 3c and d, several cuts in energy of the figure of merit for Co/W(110) and Fe/W(110) are shown, respectively. The FOM of Co/W(110) displays a pronounced maximum of 0.02 for 5 ML film thickness at an electron kinetic energy of 2 eV. In Fe/W(110) we have found a maximal FOM of 0.01 at 3.2 eV for 4 ML film thickness. These results clearly show that the Co/W(110) thin film gives higher value of FOM than the Fe/W(110) thin film when the films are grown at room temperature.

We also address a known difficulty in exchange-scattering polarimetry related to surface conditions of the magnetic films used. Over the course of many hours or days, adsorption of contamination from rest-gas present in UHV considerably reduces both the reflectivity and the spin asymmetry of the film (aging effects). In a spin-detector application such aging effects cause degradation of the FOM over time and therefore cause considerable losses of efficiency. To fully characterize the Co/W(110) 5 ML thin film (the one leading to the highest FOM), we have performed a detailed time and annealing temperature dependence of the reflectivity. For this purpose, freshly grown films were stored in an annex chamber with a base pressure of $2\text{x}10^{-9}$ Torr to study the effects of UHV contamination.

Figure 4a and b shows how the high reflectivity and asymmetry of a 5 ML thick Co film, measured every 24 hours for 3 days, evolve with time. One can see that already after 24 hours the reflectivity is substantially suppressed, the spin asymmetry is reduced by 50%, and the maximum FOM is diminished by almost 90%. We found that this aging effect can be easily reversed with a thermal treatment. Figures 4c and d show how careful annealing leads to substantial recovery of the film's original exchange-scattering characteristics (75% of the original FOM). Additional heating ($T \geqslant 330°$ C.) cause the disruption of the film with the formation of 3 dimensional islands surrounded by a thin pseudomorphic film (Stranski-Krastanov film morphology). On the other hand, the effect of UHV contamination on iron is even more severe, and the FOM could not be significantly recovered by annealing before film disruption. Neither film's FOM could be recovered after exposure to atmosphere.

A complete characterization would require the incident angular acceptance of both systems, but it cannot be measured by Low Energy Electron Microscopy where only backscattering of normal incident electrons is measured. Nevertheless the angular spread of electron is by definition very small in Angle Resolved Photoemission Spectroscopy, particularly with high efficiency electron spectrometers like time of flight spectrometers[21].

IV. SUMMARY AND CONCLUSIONS

In conclusion, we presented a comparative analysis of the figure of merit as a function of thickness, energy and time of two promising thin films systems using a innovative technique based on spin polarized low energy electron microscopy. We have shown that Co/W(110) thin film is an ideal system for exchange-scattering based electron spin polarimetry, giving a figure of merit as high as 0.02 with very low stray fields and thus without spurious asymmetry. In addition, because of the homogeneity of Co/W(110) thin films grown at room temperature and the possibility of reversing aging effects by moderate annealing, this system appears particularly stable for spin polarimetry applications.

Acknowledgments

We thank G.-H. Gweon, M. Portalupi and Z. Q. Qiu for helpful discussions. This work was supported by the Director, Office of Science, Office of Basic Energy Sciences, Division of Materials Sciences and Engineering, of the U.S. Department of Energy under Contract No. DE-AC03-76SF00098. We acknowledge the support of the National Science Foundation through Grant No. DMR-0349361, the A. P. Sloan Foundation and the Hellman Foundation.

* Electronic address: jeff.graf@a3.epfl.ch

[1] J. Kessler, *Polarized electrons* (Springer-Verlag, Berlin ; New York, 1985).

[2] D. T. Pierce, R. J. Celotta, M. H. Kelley, and J. Unguris, Nucl. Instr. and Meth. A **266**, 550 (1988), URL http://dx.doi.org/10.1016/0168-9002(88)90445-7.

[3] G. Fashold, M. S. Hammond, and J. Kirschner, Solid State Commu. **84**, 541 (1992), URL http://dx.doi.org/10.1016/0038-1098(92)90186-D.

[4] F. U. Hillebrecht, R. M. Jungblut, L. Wiebusch, C. Roth, H. B. Rose, D. Knabben, C. Bethke, N. B. Weber, S. Manderla, U. Rosowski, et al., Rev. Sci. Inst. **73**, 1229 (2002), URL http://dx.doi.org/10.1063/1.1430547.

[5] R. Jungblut, C. Roth, F. U. Hillebrecht, and E. Kisker, Surf. Sci. **269-270**, 615 (1992), URL http://dx.doi.org/10.1016/0039-6028(92)91320-B.

[6] M. Hammond, G. Fahsold, and J. Kirschner, Phys. Rev. B **45**, 6131 (1992), URL http://link.aps.org/abstract/PRB/v45/p6131.

[7] R. Bertacco and F. Ciccacci, Surf. Sci. **419**, 265 (1999), URL http://dx.doi.org/10.1016/S0039-6028(98)00805-X.

[8] R. Bertacco, M. Merano, and F. Ciccacci, Applied Physics Letters **72**, 2050 (1998), URL http://link.aip.org/link/?APL/72/2050/1.

[9] R. Bertacco, M. Marcon, G. Trezzi, L. Duo, and F. Ciccacci, Review of Scientific Instruments **73**, 3867 (2002), URL http://link.aip.org/link/?RSI/73/3867/1.

[10] R. Zdyb and E. Bauer, Surf. Rev. Lett. **9**, 1485 (2002), URL http://dx.doi.org/10.1142/S0218625X02003925.

[11] R. Zdyb and E. Bauer, Physical Review Letters **88**, 166403 (pages 4) (2002), URL http://link.aps.org/abstract/PRL/v88/e166403.

[12] E. Bauer, T. Duden, and R. Zdyb, J. Phys. D **35**, 2327 (2002), URL http://dx.doi.org/10.1088/0022-3727/35/19/301.

[13] U. Gradmann and G. Waller, Surf. Sci. **116**, 539 (1982), URL http://dx.doi.org/10.1016/0039-6028(82)90363-6.

[14] T. M. Gardiner, Thin Solid Films **105**, 213 (1983), URL http://dx.doi.org/10.1016/0040-6090(83)90287-0.

[15] E. Bauer, J. Phys. C **11**, 9365 (1999), URL http://dx.doi.org/10.1088/0953-8984/11/48/303.

[16] T. Scheunemann, R. Feder, J. Henk, E. Bauer, T. Duden, H. Pinkvos, H. Poppa, and K. Wurm, Solid State Commu. **104**, 787 (1997), URL http://dx.doi.org/10.1016/S0038-1098(97)00357-8.

[17] H. J. Elmers, J. Hauschild, H. Fritzsche, G. Liu, U. Gradmann, and U. Kohler, Phys. Rev. Lett. **75**, 2031 (1995), URL http://link.aps.org/abstract/PRL/v75/p2031.

[18] D. P. Pappas, K.-P. Kamper, B. P. Miller, H. Hopster, D. E. Fowler, C. R. Brundle, A. C. Luntz, and Z.-X. Shen, Phys. Rev. Lett. **66**, 504 (1991), URL http://link.aps.org/abstract/PRL/v66/p504.

[19] F. Passek, M. Donath, and K. Ertl, J. Magn. Magn. Mater. **159**, 103 (1996), URL http://dx.doi.org/10.1016/0304-8853(95)00940-X.

[20] M. Getzlaff, J. Bansmann, and G. Schönhense, Solid State Commu. **87**, 467 (1993), URL http://dx.doi.org/10.1016/0038-1098(93)90799-S.

[21] O. Hemmers, S. B. Whitfield, P. Glans, H. Wang, D. W. Lindle, R. Wehlitz, and I. A. Sellin, Review of Scientific Instruments **69**, 3809 (1998), URL http://dx.doi.org/10.1063/1.1149183.